Conformational Isomerization of 5-Phenyl-1-pentene Probed by SEP-Population Transfer Spectroscopy

Nathan R. Pillsbury and Timothy S. Zwier*

Department of Chemistry, Purdue University, 560 Oval Drive, West Lafayette, Indiana 47907

Received: July 28, 2008; Revised Manuscript Received: October 7, 2008

Stimulated emission pumping-population transfer (SEP-PT) spectroscopy is used to experimentally determine upper and lower bounds on the energy thresholds to conformational isomerization between 14 X→Y reactant−product conformer pairs of isolated 5-phenyl-1-pentene (5PPene). This work builds directly on the spectroscopic assignments of the five observed conformers of 5PPene in the preceding paper. The observed thresholds fall into two energy ranges: near 600 cm^{-1} for isomerization processes that involve only reorientation of the terminal vinyl group, and in the 1200−1374 cm^{-1} range for barriers that involve hindered rotation about the alkyl chain carbon−carbon bonds. As a result, this latter threshold opens up much of the conformational phase space to exploration, with multiple isomerization pathways connecting any two of the conformational minima.

I. Introduction

In the preceding paper,[1] the conformation-specific spectroscopy of the alkylbenzene, 5-phenyl-1-pentene (5PPene, Figure 1), was discussed. Five conformational isomers, labeled A−E, were observed in the free jet environment with S_0-S_1 origin transitions at 37 518, 37 512, 37 526, 37 577, and 37 580 cm^{-1}, respectively. Rotational band contour analysis provided a basis for firm assignments of four of the five conformers, with the fifth constrained to one of two possibilities. These structures are shown next to their corresponding origin transitions in Figure 2. The labeling scheme for the structures[1] identifies the local configuration of each of three dihedral angles along the pentene chain (τ_1 about the $C_\alpha-C_\beta$ bond, τ_2 about the $C_\beta-C_\gamma$ bond, and τ_3 about the $C_\gamma-C_\delta$ bond) which serve as the principal flexible coordinates. The $C(1)-C_\alpha$ dihedral is near 90° in all the low-energy structures.

While spectroscopy tends to focus attention on the minima, where the population resides, the kinetics and dynamics of isomerization are determined by the energy barriers that separate these minima. One is naturally led, then, from a consideration of the conformational preferences of 5-phenyl-1-pentene to its isomerization. Experimental studies of these regions of the potential energy surface, while of great importance, lag far behind those on the minima.

Knowledge of the energy barriers to isomerization has significant consequences in a range of contexts. First, one of the motivations for the study of the spectroscopy of 5-phenyl-1-pentene[1] was that the photophysics and photochemistry of the molecule involved exciplex formation between the phenyl ring and vinyl groups, which should have different energy thresholds in the excited state depending on starting conformation. We argued in that work[1] for the transferability of ground state barriers in the pentene chain (determined in this paper) to the S_1 state, providing a rationalization for the precipitous drop in S_1 lifetimes at a threshold of ~1000 cm^{-1}. Second, those seeking to understand the conformational dynamics of liquid alkanes,[2,3] self-assembled monolayers,[4] membranes,[5,6] and other environments in which alkyl or alkenyl chains are involved require as fundamental input isomerization barrier height to understand the types and time scales governing their motions. Finally, the alkylbenzenes themselves are significant constituents in gasoline and diesel fuels,[7,8] and models of their combustion must necessarily take into account the presence and interconversion of conformational isomers, which modulate the distance between reacting segments of the molecule.

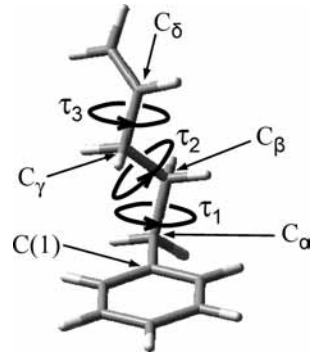

Figure 1. Example structure of 5PPene with relevant atoms and dihedral angles labeled.

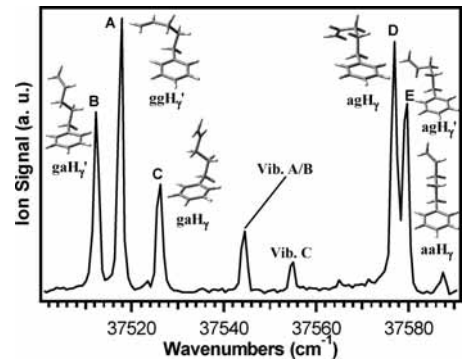

Figure 2. R2PI of the 5PPene origin region (37 000−37 590 cm^{-1}) with corresponding assigned structures. Both possible structures of conformer E are shown.

* To whom correspondence should be addressed. E-mail: zwier@purdue.edu.

10.1021/jp806699e CCC: $40.75
Published on Web 12/09/2008

To carry out a conformation-specific study of isomerization, an experimental method is required that (i) is capable of selective excitation of a single conformational isomer, (ii) incorporates a means of tuning the energy content of the isomer, and (iii) provides selective detection of the population change induced in each conformational product. We have recently introduced a method that meets each of these criteria, called stimulated emission pumping-population transfer spectroscopy.[9−16] Here we apply this method to determine the energy thresholds to isomerization in 5PPene.

In 5PPene, an immediate challenge arises simply from the fact that there are five observed conformers even under jet-cooled conditions, so a complete isomerization study would need to consider the entire set of 20 independent X→Y reactant−product pairs. Additional complexity comes from the fact that the observed minima have spectroscopically indistinguishable mirror images that also contribute to the isomerization pathways. In the present work, we apply the method of stimulated emission pumping-population transfer (SEP-PT) spectroscopy to 5PPene. The method builds off the single-conformation spectroscopy in the preceding paper, which provided unique spectral signatures that can be used to study conformational isomerization and provides a means for addressing the three criteria above. SEP-PT combines an initial cooling step in the supersonic expansion with SEP excitation to selectively excite conformer X to a ground state energy level with well-defined, but tunable internal energy, thereby initiating conformational isomerization. Population transferred between X and Y is detected as a gain in the fluorescence signal from a probe laser positioned downstream in the expansion, where collisional cooling has repopulated the zero-point levels of reactant and products.

This paper reports a study of 14 of the 20 X→Y conformer pairs with SEP-PT spectroscopy. Lower and upper bounds are placed on the energy thresholds to isomerization between these pairs. These thresholds are associated with the rate-limiting energy barriers along the pathways that lead from reactant to product. As we shall see, certain of the reactant−product pairs involve motion primarily along a single dihedral angle, thereby mapping directly onto these barriers. We use the set of results to test two often-used density functional theory methods,[17−19] advocating for the inclusion of experimental results of this type in future test sets of computational methods. The entire data set provides a picture of isomerization in 5PPene in terms of successions of one-dimensional hindered rotations, with a ∼1200 cm^{-1} threshold opening up access to a wide range of conformational space that includes all five of the observed conformational wells.

II. Methods

A. Experimental Details. The laser induced fluorescence (LIF) apparatus utilized in this experiment has been described elsewhere.[20] A total pressure of 3 bar of helium was passed through a heated sample reservoir (35 °C) containing 5PPene. The gaseous sample was then injected into a vacuum chamber via a pulsed General Valve (Series 9, 20 Hz) with a 1.2 mm orifice diameter, cooling the molecules to their zero-point vibrational levels (ZPL). SEP spectra were recorded in the collision-free region of the expansion, ∼1 cm from the nozzle orifice. The cold molecules were excited to the first excited state by a UV laser (pump laser, ∼0.3 mJ/pulse, 20 Hz) fixed at a frequency corresponding to a particular transition in the LIF spectrum (usually the S_0-S_1 origin). Immediately following excitation (∼5−6 ns later), a second UV laser (dump laser, ∼1.5 mJ/pulse, 10 Hz) was used to stimulate emission back to the ground state. When the dump laser is scanned and becomes resonant with an SEP transition, a dip in the total fluorescent signal from the pump laser is detected. Conformation-specific stimulated emission pumping (SEP) spectra were recorded by plotting the averaged output of the gated integrator (in active baseline subtraction mode) versus the frequency of the dump laser. These SEP spectra were a prerequisite for the SEP-PT experiment discussed below.

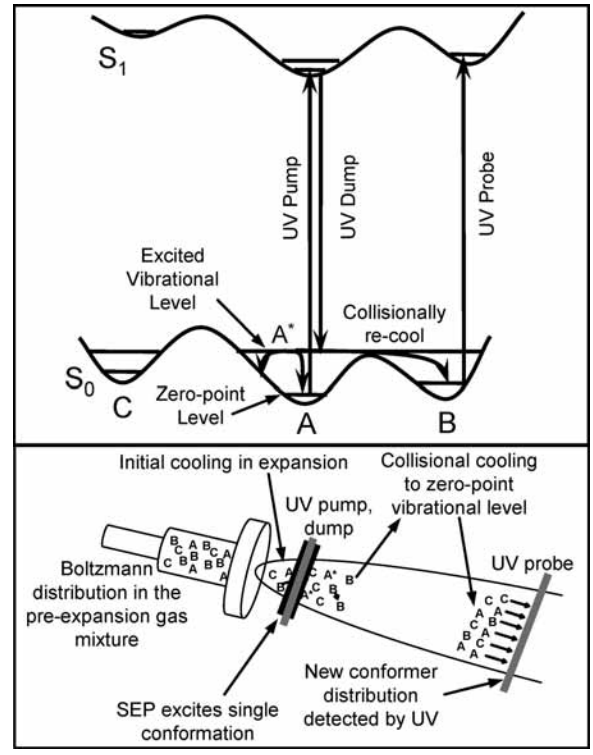

Figure 3. Top: Potential energy diagram of the SEP-PT experiment. Bottom: Schematic of the experimental setup.

Stimulated emission pumping-population transfer spectroscopy (SEP-PTS) is a powerful spectroscopic technique that was developed in our laboratory.[9−16] This method can be used to experimentally determine the barriers to isomerization between reactant−product pairs of conformationally flexible molecules. A schematic potential energy diagram and experimental setup are shown in Figure 3. After initial cooling with helium (∼6 bar) to the ZPL, an SEP step is performed early in the supersonic expansion ($x/d \approx 5$, x = distance from nozzle, d = nozzle orifice diameter = 1.2 mm) to put population into a well-defined S_0 energy level. The wavelength of the pump laser (∼0.4−0.5 mJ/pulse, 20 Hz) is fixed on a vibronic band (usually the S_0-S_1 origin) of the reactant conformation. The dump laser (∼0.5−1.0 mJ/pulse, 10 Hz) is scanned and stimulates population down to vibrational levels in the ground state, thereby initiating conformational isomerization when energetically feasible. The SEP-excited molecules are given time (∼2 μs) to collisionally recool back to the ZPL where they are probed by a third UV laser (∼0.2−0.3 mJ/pulse, 20 Hz, $x/d \approx 8$). The probe laser is either set to monitor the reactant or a specific product conformer population, using its S_0-S_1 origin transition. If the dump laser stimulates population down to a ground state level that is below the barrier to isomerization, the molecules so excited can only cool back to the ZPL of the reactant well. However, if the energy given is enough to surpass the barrier, some of the molecules may isomerize and be cooled down to the ZPL of the product well. By recording the integrated LIF signal from the probe laser in a 20 Hz pump/10 Hz dump/20 Hz probe

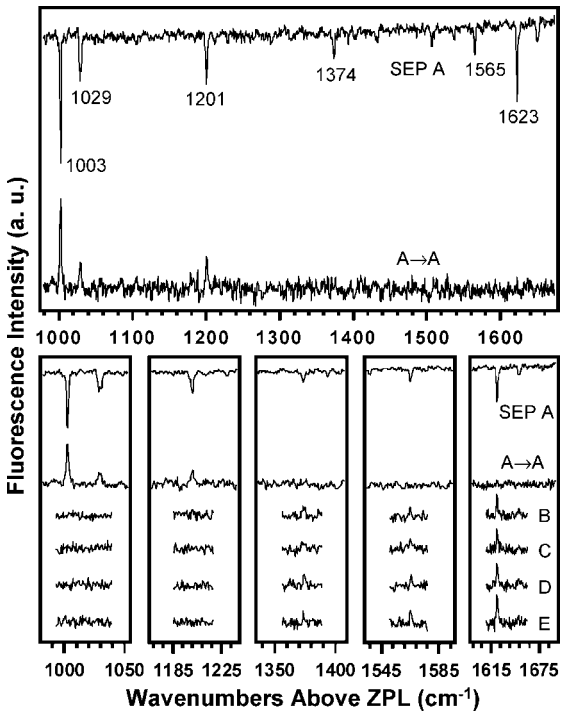

Figure 4. SEP and SEP-PT spectra out of conformer A. The key transitions have been labeled in the SEP spectrum of the top graph with their respective frequency values (in cm^{-1}) from the ZPL. The bottom set of graphs are expanded views of the SEP-PT spectra out of A to the indicated products (A−E).

configuration using active baseline subtraction, the difference signal reflects the population change induced by the dump laser. Whether the population change in reactant X or product Y is detected, a gain is observed in the signal from the probe laser, reflecting an increase in population accompanying the action of the dump laser. Collecting the integrated signal from the probe laser and plotting it versus the dump wavelength yields the SEP-PT spectra. Comparing these spectra to the SEP spectra allows for the determination of lower and upper bounds on the barrier to X→Y isomerization. The first SEP transition in which a gain in product Y population is observed gives an upper bound to the barrier, while the last transition that is not seen gives the lower bound. By measuring the barriers to the forward and reversed reactions between two reactant/product pairs (A→B, B→A), a range on the relative energies of the minima can also be determined.

B. Computational Methods. The results of ground state optimizations performed at the DFT Becke3LYP[17,18]/6-31+G*, MP2[21−26]/6-311++G**, and DFT M05-2X[19]/6-31+G* levels of theory were reported in the preceding paper.[1] These results will be useful when predicting the barrier heights of specific X→Y isomerizations. QST3 transition state calculations were performed by using DFT B3LYP/6-31+G* and M05-2X/6-31+G* levels of theory. All calculations were performed with use of the Gaussian 03 computational package.[27]

III. Results and Analysis

Figure 4 presents the SEP and SEP-PT spectra out of conformer A (ggH_γ'). In these scans, the ordinate is the difference in photon energies of the pump and dump lasers (in cm^{-1}), plotted so as to report directly the initial energy of the reactant conformer produced by the SEP transition back to the ground state. The top trace in the upper figure is the SEP spectrum, recorded as a depletion in the fluorescence signal from the pump laser caused by the dump laser. As expected, there are comparatively few strong SEP transitions in the 980−1680 cm^{-1} region, because the Franck−Condon factors that govern the SEP transitions are those expected for substituted benzenes, most particularly toluene. In 5PPene, the longer alkene chain does not significantly perturb these Franck−Condon factors nor does it turn on low-frequency transitions involving the alkene chain itself.

The full A→A "reactant" SEP-PT spectrum is shown directly below the SEP spectrum for comparison. At internal energies of A up to ∼1300 cm^{-1} above its ZPL, this spectrum shows gains at the positions of all the SEP transitions with their correct relative intensities. However, above this energy, the gains cut off sharply. This loss in signal intensity is indicative of overcoming one or more barriers to isomerization near 1300 cm^{-1}.

Close-up views of the entire set of SEP and SEP-PT spectra are shown in the lower half of the figure. The SEP-PT spectra out of A monitoring products B−E were recorded only in small energy regions around the strong SEP transitions. This was done in order to focus attention on the relevant energy windows where transitions are anticipated, a necessary strategy given the low signal levels involved. As Figure 4 shows, the SEP-PT spectra from A to the other conformers (labeled B−E) all show nearly identical behavior. Transitions at 1003, 1029, and 1201 cm^{-1} are missing from the product SEP-PT spectra, as they should be if there is insufficient energy to isomerize. However, all four product spectra show a sharp onset of gains beginning with the transition at 1374 cm^{-1}, and including all transitions higher in energy (1565 and 1623 cm^{-1}). We surmise on this basis that 1374 cm^{-1} is the upper bound to the energy threshold for all four of these A→X product spectra, while 1202 cm^{-1} is a lower bound. This finding is consistent with the sudden drop in gain signal in the A→A spectrum at this same threshold, since the population is being siphoned out of A and into all of the other conformations at energies above this threshold. In the absence of tunneling or kinetic shifts, these bounds bracket the classical energy barrier separating A from each of the products B−E.

Figure 5 shows the SEP and SEP-PT spectra out of conformer B (gaH_γ'). Only the SEP-PT spectra of B→B, B→C, and B→D gave sufficient gain signal to discern energy thresholds, and therefore only those scans are plotted. In keeping with expectation, at low energies clear gains are observed in the B→B reactant spectrum, followed by a sharp cutoff as energy thresholds to isomerization are overcome. In this case, the cutoff occurs between 1003 and 1031 cm^{-1}, almost 200 cm^{-1} below that in the A→A spectrum (Figure 4). Interestingly, the B→C SEP-PT spectrum shows a clear gain signal already at the lowest energy transition observed in the B SEP spectrum, at 622 cm^{-1}. All transitions above this energy also show a gain signal, indicating that the energy threshold for B→C isomerization is below 622 cm^{-1}. A firm lower bound cannot be determined due to lack of vibronic activity below 622 cm^{-1}. Nevertheless, an argument can be made that the 622 cm^{-1} SEP transition is just above threshold, based on the observed SEP-PT transition intensities. In particular, the intensity of the 622 cm^{-1} transition in the B→C spectrum is about one-third the size of the same transition in the B→B spectrum, while higher energy transitions at 751 and 809 cm^{-1} have intensities similar to those in the B→B spectrum. This suggests that the barrier to B→C isomerization has just been exceeded at 622 cm^{-1}, so that vibrational cooling back into the reactant well (B) occurs in competition with isomerization to C. As we shall see shortly, this competition is anticipated only in a narrow energy window immediately

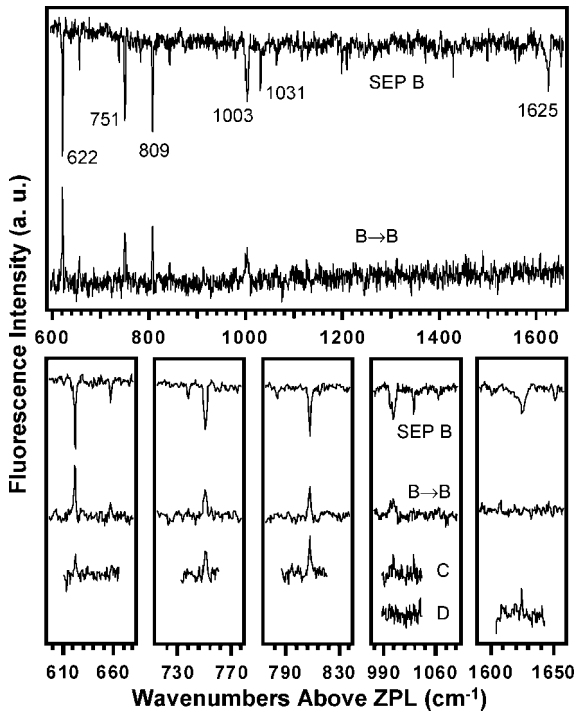

Figure 5. SEP and SEP-PT spectra out of conformer B. The key transitions have been labeled in the SEP spectrum of the top graph with their respective frequency values (in cm^{-1}) from the ZPL. The bottom set of graphs are expanded views of the SEP-PT spectra out of B to the indicated products (B, C, and D).

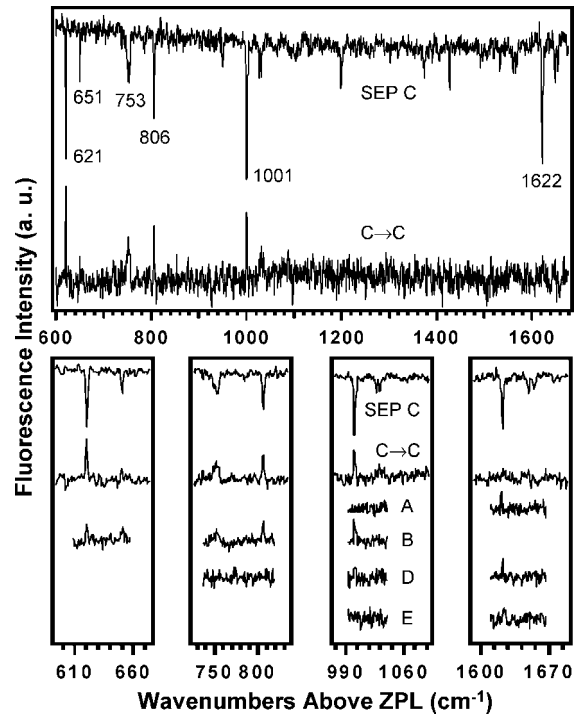

Figure 6. SEP and SEP-PT spectra out of conformer C. The key transitions have been labeled in the SEP spectrum of the top graph with their respective frequency values (in cm^{-1}) from the ZPL. The bottom set of graphs are expanded views of the SEP-PT spectra out of C to the indicated products (A−E).

above threshold. While the reactant spectrum shows evidence that the barrier to other products occurs near 1030 cm^{-1}, clear evidence for this fact in the other product spectra could not be obtained. Only in the B→D spectrum was it possible to clearly see the onset of product gain signal, and there only at the intense SEP transition at 1625 cm^{-1}, thereby placing very large bounds on the B→D isomerization threshold between 1003 and 1625 cm^{-1}.

The SEP and SEP-PT spectra out of conformer C (gaH_γ) are shown in Figure 6. Again the intensity of the reactant (C→C) gain signal drops off suddenly near 1000 cm^{-1}, with the intensity of the transition at 1001 cm^{-1} was reduced relative to lower energy transitions, suggesting that one or more barriers are opening up close to this energy. Like the B→C spectrum in Figure 5, the C→B spectrum shows gains from the lowest energy transition at 621 cm^{-1}. The decreased intensity of the 621 cm^{-1} transition in the C→B spectrum (compared to the same transition in the reactant C→C spectrum) points once again to this transition being just above the energy threshold for C→B isomerization. On the basis of the other product SEP-PT spectra in Figure 6, the barriers out of C to the other conformers (A, D, and E) could only be set between 1001 and 1622 cm^{-1}.

Figure 7 shows the SEP and SEP-PT spectra out of conformer D (agH_γ). Once again the reactant intensity drops off near 1000 cm^{-1} above the zero-point level. Clear gain signals are observed in product spectra out of D to the other four conformers (A, B, C, and E) only at 1624 cm^{-1}, leading to large limits on the isomerization thresholds out of D (between 1002 and 1624 cm^{-1}). Finally, the SEP-PT spectrum out of conformer E (agH_γ' or aaH_γ) in Figure 8 shows the same drop-off in the E→E spectrum above ~1000 cm^{-1}. In this case, signal levels prevented measurement of barriers out of E to any of the other conformations.

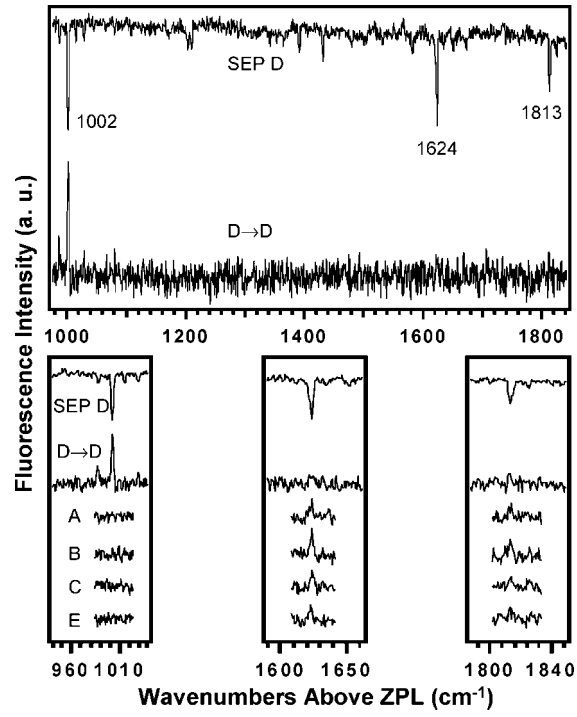

Figure 7. SEP and SEP-PT spectra out of conformer D. The key transitions have been labeled in the SEP spectrum of the top graph with their respective frequency values (in cm^{-1}) from the ZPL. The bottom set of graphs are expanded views of the SEP-PT spectra out of D to the indicated products (A−E).

IV. Discussion

The laser-based, triple resonance method of stimulated emission pumping-population transfer spectroscopy has been used to place experimental bounds on the barriers to isomer-

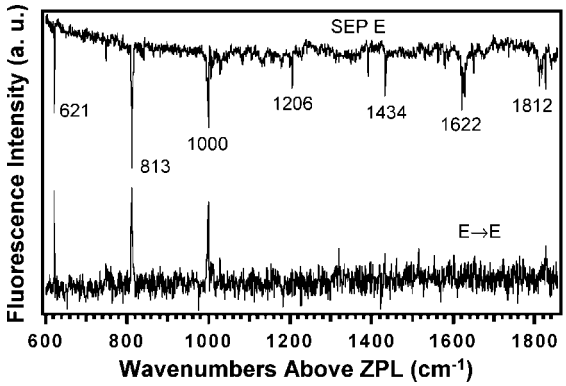

Figure 8. SEP and SEP-PT spectra out of conformer E. The major transitions are labeled with their respective positions from the ZPL in wavenumbers (cm^{-1}).

TABLE 1: Zero-Point Corrected, Relative Energies of the Five Conformations of 5PPene As Predicted by DFT B3LYP and M05-2X Methods, as Well as the Relevant Dihedral Angles

conformer	B3LYP/ 6-31+G* (cm^{-1})	M05-2X/ 6-31+G* (cm^{-1})	τ_1°	τ_2°	τ_3°
A (ggH_γ')	448	0	−67	−67	126
B (gaH_γ')	238	147	−65	179	118
C (gaH_γ)	270	158	−65	−176	−121
D (agH_γ)	144	95	180	67	−122
E1 (aaH_γ)	0	130	180	−178	−120
E2 (agH_γ')	347	410	177	64	115

ization between the five observed conformations of 5-phenyl-1-pentene. 5PPene was chosen in part because it was a model alkenylbenzene closely analogous to the molecules studied in some detail previously by Smalley and co-workers in the context of their ground-breaking work on intramolecular vibrational redistribution (IVR).[28−30] Since the SEP transitions used in this work involve ground state levels that are largely localized on the phenyl ring of 5PPene, IVR to the torsional levels is a prerequisite for conformational isomerization. In this sense, having both types of measurements on similar systems provides a solid experimental foundation for theoretical investigations of the isomerization dynamics.

A. Evaluating the DFT Calculations. Table 1 summarizes the relative energies of the minima (in cm^{-1}) and the values of the dihedral angles for each of these structures at the DFT B3LYP/6-31+G* and DFT M05-2X/6-31+G* levels of theory. They are reproduced here in order to facilitate a comparison with the calculated conformational transition states of relevance in this work.

1. Barrier Heights. One of the stated goals for this work is to provide experimentally measured barrier heights and relative energies of the minima that could be used to test theoretical methods for their evaluation. The experimental energy thresholds listed in Table 2 provide a basis for such comparison. The experimental data set includes measurements of 14 independent X→Y thresholds. Of this 14, those providing the most critical tests of theory are the four thresholds out of the conformer A well (for which we have fairly narrow bounds), and the B↔C pair. We were only able to place lower and upper bounds between 1000 and 1620 cm^{-1} in most of the other cases. These threshold measurements suffer from what can be a significant limitation of the SEP-PT method, which relies on the presence of SEP transitions with large Franck−Condon intensity to prepare the ground state levels for study. In 5PPene, the toluene-like vibronic structure is quite sparse, leading to significant energy gaps. Furthermore, the oscillator strength of the S_0-S_1 transition in 5PPene is rather weak, making it difficult to drive sufficient population back to the ground state level(s) to observe weak transitions in the SEP spectrum.

TABLE 2: Comparison between the Experimentally Determined and Predicted Thresholds to Isomerization of 5PPene[a]

barrier	expt (cm^{-1})	B3LYP/ 6-31+G* (cm^{-1})	M05-2X/ 6-31+G* (cm^{-1})	$C_\alpha-C_\beta$ (τ_1)	$C_\beta-C_\gamma$ (τ_2)	$C_\gamma-C_\delta$ (τ_3)
A→B	1202−1374	936	1347		X	
A→C	1202−1374				X	X
A→D	1202−1374			X	X	X
A→D_m		857	1269	X		
A→E1	1202−1374			X	X	X
A→E2				X	X	
B→C	<622	646	676			X
B→D	1003−1625			X	X	X
C→A	1001−1622				X	X
C→B	<621	616	671			X
C→D	1001−1625			X	X	
C→E1	1001−1622	927	1216	X		
C→E2				X	X	X
D→A	1002−1624			X	X	X
D_m→A				X		
D→B	1002−1624			X	X	X
D→C	1002−1624			X	X	
D→E1	1002−1624	918	1138		X	
D→E2		527	957			X

[a] Also, indicated by an "X" are the C−C bonds for which a rotation is needed to isomerize from reactant to product. The forward and reverse reactions from A to D and also to its mirror image (D_m) are given in order to compare their isomerization pathways.

To make a quantitative comparison between experiment and theory, the observed energy thresholds must faithfully represent lower and upper bounds on the classical energy barriers themselves. This assumes that neither kinetic shifts (yielding a threshold higher in energy than the barrier) nor tunneling effects (which could be responsible for a threshold below the classical barrier) are significant. Tunneling would seem not to be a problem in 5PPene, in that isomerization involves motion of one or more heavy atoms in all cases. A kinetic shift would occur if the rate of isomerization at threshold were slow compared to the collisional cooling rate at the point of SEP excitation. To assess this possibility, we must compare the 5PPene-He collision rate with the threshold isomerization rate, calculated using RRKM theory.[31,32] The rate of collisions with helium was estimated at the point of SEP excitation by using a hard-sphere model developed by Lubman et al.[33] to describe collisions in a supersonic expansion. The collision rate, z_{jet} (collisions/s), is given by

$$z_{jet} = (2)^{1/2} n_0 \sigma v_0 \left[1 + \frac{1}{2}(\gamma - 1) M_{eff}^2\right]^{(-1/2)[(\gamma-)/(\gamma+)]} \quad (1)$$

where n_0 is the reservoir density, $\bar{v}_0$ is the mean velocity in the reservoir, γ is the heat capacity ratio C_p/C_v of the main expansion gas (helium, $C_p/C_v = 5/3$), and M_{eff} is the local Mach number. From these values the collision rate was estimated to be $\sim 7 \times 10^7\ s^{-1}$ at $x/d = 5$, where SEP occurs in the present experiment. According to RRKM theory, the isomerization rate is given by

$$k_{isom}(E) = N^{\ddagger}(E - E_0)/h\rho(E) \quad (2)$$

where $N^{\ddagger}(E - E_0)$ is the number of states available at energy E to the transition state, h is Planck's constant, and ρ(E) is the

vibrational density of states of the reactant at energy E. At threshold, $N^{\ddagger}(E - E_0) = 1$. For conformer A of 5PPene at an energy $E = 1350$ cm^{-1}, $k_{isom} = \sim 3 \times 10^7$ s^{-1}, which is within a factor of 2 of the collision rate. This means that already at threshold, isomerization competes effectively with collisional cooling. Furthermore, based on a recent study of bis(2-hydroxyphenyl)methane,[14] we anticipate that each 5PPene-He collision will remove on average $\sim$10−15 cm^{-1} in this energy range. We thus estimate a kinetic shift of no more than 50 cm^{-1} in the observed thresholds. Since the smallest energy gap between lower and upper bounds is about 170 cm^{-1}, a kinetic shift of this magnitude would be negligible.

To make the comparison between experiment and theory, it is also essential to associate the correct theoretical transition state with that responsible for the energy threshold observed experimentally. The torsional surface of relevance for near-threshold isomerization involves motion along the three torsional dihedrals that flex the pentene chain: τ_1, τ_2, and τ_3 (Figure 1). A more detailed assessment of the multidimensional potential energy surface and the isomerization pathways on it will be taken up shortly. However, for the purpose of comparison between experiment and theory, we consider here only those reactant−product pairs for which the transition state differs from reactant and product primarily along a single torsional coordinate: A→B (τ_2), A→D$_m$ (τ_1), and B→C (τ_3).

Table 2 compares the measured energy thresholds for these three reactant−product isomerization pairs with the results of DFT calculations using the B3LYP and M05-2X functionals, both with the 6-31+G* basis set. As can be seen from this comparison, the predictions of the DFT M05-2X calculations are in better quantitative agreement with experiment, especially for the barriers out of conformer A (ggH$_\gamma'$). This is most likely because "A" is a *gauche−gauche* structure, whose folded geometry leads to substantial dispersive interactions between the segments of the pentene side chain and between the pentene chain and the ring. One of the well-documented deficiencies of the B3LYP functional is its incorrect description of dispersive interactions, which are systematically underestimated.[34,35] In keeping with this, the calculated barriers out of A are systematically too small with DFT B3LYP, because the ggH$_\gamma'$ structure is not stabilized sufficiently by such interactions relative to the other minima (Table 1). Among the attempted solutions to this deficiency are new functionals designed to better account for dispersion.[19,35−39] One of the recent entries in this category is a functional developed by Truhlar and co-workers, M05-2X.[19,35,39] Recent studies have shown that this functional predicts relative energies of minima and barrier heights in closer correspondence with experiment, and therefore accounts for dispersive interactions better than many other functionals.[14,40] The present results on 5PPene add further experimental evidence to this deduction. Tests with larger basis sets indicate that this discrepancy cannot be removed simply by increasing the size of the basis set.

2. The Relative Energies of the Minima. By measuring both the X→Y and Y→X isomerization thresholds one can obtain the relative energies of the minima by subtracting the two barriers from one another: $E_{thresh}(X\rightarrow Y) = E(\text{barrier}) - E_X$, $E_{thresh}(Y\rightarrow X) = E(\text{barrier}) - E_Y$, $\Delta E_{XY} = E_{thresh}(X\rightarrow Y) - E_{thresh}(Y\rightarrow X)$. In cases where the experimental bounds placed on the energy thresholds were rather large, it leads to an even larger range of values for ΔE_{XY} with comparably little quantitative information content. However, the measured threshold between B and C did shed some light on this subject. It was determined from the relative sizes of the transitions in the B→C and C→B SEP-PT spectra that the barriers were both just under $\sim$620 cm^{-1}. Since the two thresholds were measured to be close to the same, the relative energies of B and C must be nearly degenerate. This provides some evidence that M05-2X is closely predicting these values because it also predicts that conformers B and C are nearly degenerate (Table 1).

We recommend the incorporation of the present results and others like it[14,16,20,41−45] in which conformer-specific spectroscopy is used to determine the number of conformations present, their assignments, and (where possible) relative energies of the minima and isomerization barriers separating them in future sets of molecules used to test theoretical methods seeking a quantitative account of dispersive and H-bonding interactions.[19,36,39,46,47]

B. Isomerization Pathways. As Table 2 indicates, many of the reactant−product pairs for which we have experimental data involve changes in more than one of the three principal dihedral angles associated with the pentene chain: (τ_1, τ_2, τ_3). All five of the observed conformers of 5-PPene have the C$_\alpha$−C$_\beta$ bond nearly perpendicular to the ring; furthermore, the barrier to isomerization about this bond is calculated to be about 2000 cm^{-1}. Therefore, hindered rotation about the C(1)−C$_\alpha$ bond is not expected to be significant in the threshold energy range. Our discussion of conformational isomerization can thus focus primarily on motion on a 3D torsional surface involving τ_1, τ_2, and τ_3. The experimental data provide a measurement of a single energy threshold for each reactant−product pair. Ideally, one would like to connect the experimental thresholds to specific stationary points on the potential energy surface. Furthermore, by linking together such measurements, we hope to learn about the efficient isomerization pathways on the potential energy surface.

Before taking up this discussion of isomerization pathways, it is first necessary to briefly discuss two aspects of the multidimensional potential energy surface which have not yet been fully addressed. First, each conformational minimum can exist in one of two mirror images which can be interconverted by reflecting through a plane perpendicular to the plane of the aromatic ring that includes the C(1)−C$_\alpha$ bond (Figure 1). To convert between mirror image structures, the dihedral angles describing the pentene chain (τ_1, τ_2, τ_3) must be inverted to ($-\tau_1$, $-\tau_2$, $-\tau_3$). At the resolution of the spectroscopic measurements carried out in the preceding paper,[1] tunneling splittings for interconversion between these mirror images are unresolved, and a single minimum could be considered. However, when considering isomerization pathways, the presence of two minima on the potential energy surface associated with each conformer can produce four pathways connecting them (X→Y, X→Y$_m$, X$_m$→Y, and X$_m$→Y$_m$, where "m" = "mirror image"), two of which may be unique. Furthermore, a given reactant and product can have distinct pathways through an intermediate conformer or its mirror image (X→Y→Z or X→Y$_m$→Z). Thus, our discussion of isomerization pathways may refer at times to pathways involving mirror image structures either as reactants, products, or intermediates.

Second, given the presence of these mirror image structures, the labeling scheme used to describe the observed conformers must be generalized to include these mirror images, which distinguishes gauche dihedrals as g$_+$ ($\tau \approx +60°$) from g$_-$ ($\tau \approx -60°$). Thus, conformer A (ggH$_\gamma$) has two mirror images: g$_+$g$_+$H$_\gamma'$ and g$_-$g$_-$H$_\gamma$. This more general labeling scheme is used in Table 3.

As Table 2 shows, experimental energy thresholds between 1200 and 1374 cm^{-1} have been determined for isomerization out of A to all the other conformers B−E. A→B isomerization involves the τ_2 dihedral only, thereby providing a direct measure

TABLE 3: Representative Calculated Transition State Structures and Relative Energies (Zero-Point Corrected) of 5PPene at the DFT M05-2X/6-31+G* Level of Theory

barrier	barrier from A (cm^{-1})	barrier from reactant (cm^{-1})	τ_1°	τ_2°	τ_3°
$g_-g_-H_\gamma'$(A)→g_-aH_γ'(B)	1347	1347	−64	−121	119
ag_+H_γ'(E2)→ag_-H_γ'	1856	1446	−177	−1	118
$g_-g_-H_\gamma'$(A)→ag_-H_γ'(D_m)	1269	1269	−120	−65	119
g_-aH_γ(C)→aaH_γ(E1)	1373	1216	−120	−178	−118
g_-aH_γ'(B)→$g_-g_-H_\gamma'$(A)	1344	1197	−64	−121	119
g_-aH_γ'(B)→g_-aH_γ(C)	823	676	−62	−177	−180
ag_+H_γ'(E2)→$g_-g_+H_\gamma'$	1905	1495	−123	68	123
g_-aH_γ'(B)→aaH_γ'	1336	1189	−121	178	119
g_-aH_γ(C)→$g_-g_-H_\gamma$	1342	1184	−64	−117	−122
g_-aH_γ(C)→g_-aH_γ'(B)	829	671	−62	−177	−180
ag_-H_γ'(D_m)→$g_-g_-H_\gamma'$(A)	1273	1178	−120	−65	119
ag_+H_γ(D)→aaH_γ(E1)	1233	1138	−179	122	−119
ag_+H_γ(D)→ag_+H_γ'(E2)	1052	957	−178	70	173
aaH_γ(E1)→g_-aH_γ(C)	1372	1242	−120	−178	−118
aaH_γ(E1)→ag_+H_γ(D)	1229	1099	−179	123	−119
ag_+H_γ'(E2)→ag_+H_γ(D)	1048	638	−178	70	173

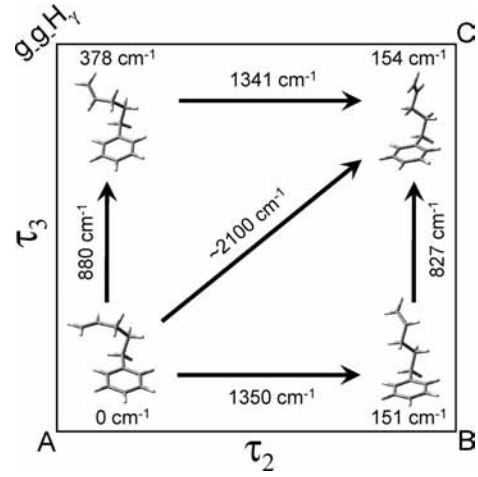

Figure 9. Representative pathways to isomerization between conformers A and C including calculated barriers and energies of the minima at the DFT M05-2X/6-31+G* level of theory, relative to A.

of the barrier to hindered rotation involving the $C_\beta-C_\gamma$ bond in the 1200−1374 cm^{-1} range. For the A→D reactant−product pair (Table 2), isomerization to the two mirror image structures of conformer D involve different pathways, with A→D requiring motion along all three dihedrals, but A→D_m only one (τ_1). This illustrates clearly the need for inclusion of mirror-image structures when considering isomerization pathways. If, as seems likely, the simple 1D motion is the preferred pathway from A to D, one can surmise that hindered rotation about the $C_\alpha-C_\beta$ bond has a similar barrier in the 1200−1374 cm^{-1} range. The experimental bounds placed on the C→E and D→E isomerizations (1000−1624 cm^{-1}) are consistent with the τ_1 and τ_2 barriers just given. On the basis of energetic grounds (Table 1), the preferred assignment for conformer E is to E1(aaH_γ), which can be formed from C and D by 1D rotation about τ_1 and τ_2, respectively. Finally, from the B↔C pair, we see that internal rotation of the vinyl group (involving τ_3), which interconverts the H_γ and H_γ' isomers, has a barrier of ∼600 cm^{-1}, only half of that for hindered rotation of the other two dihedrals τ_1 and τ_2.

All of the other reactant−product pairs involve significant changes along 2 or more dihedrals. The question is whether the minimum-energy pathway in these cases involves a series of sequential 1D hindered rotations, or a concerted motion in which more than one dihedral is rotated simultaneously. In the former case, the sequential steps would take the molecule from one minimum to the next over what are essentially one-dimensional barriers involving one of the dihedrals. The latter possibility could hold if motion along more than one dihedral angle would energetically compensate for one another. This would produce pathways that avoid intermediate minima in their traversal from reactant to product.

The experimental data point toward sequential 1D hindered rotations being operative in 5PPene. The experimental barriers for A→C (τ_2, τ_3) and A→E (τ_1, τ_2, τ_3) isomerizations are both in the same 1200−1374 cm^{-1} range as for the 1D cases of A→B (τ_2) and A→D_m (τ_1), consistent with the rate-limiting barriers for A→C and A→E being a 1D barrier closely analogous to those for A→B and A→D_m. Calculations bear this out. For instance, Figure 9 presents a two-dimensional cut of the (τ_2, τ_3) surface connecting A and C. Two nearly equivalent sequential pathways connect A and C, involving motion first along τ_2 (to minimum B) and then τ_3, or vica versa. In the former case, minimum B acts as intermediate, with its rate-limiting barrier traversed first, followed by a much lower barrier in the second step. In the (τ_3, τ_2) pathway, the $g_-g_-H_\gamma$ minimum serves as an intermediate, despite the fact that it is not one of the observed conformers. In both pathways, the rate-limiting barrier connecting A and C is nearly the same (1341 or 1350 cm^{-1}). The diagonal pathway is anticipated to traverse a second-order saddle point with energy ∼2100 cm^{-1}, roughly the sum of the two 1D barriers.

To test the generality of this deduction, we carried out transition state calculations for all 20 X→Y reactant−product pairs in 5PPene starting from guessed transition state structures with dihedrals that were the average of the starting and ending structures, that is, near the diagonal midpoint in the multidimensional pathway. Since some of the calculations optimized to the same TS structure, only the unique values are summarized in Table 3. In all cases, the located first-order transition states are 1D transition states in which two of the dihedrals are near one of their minimum-energy values (differing by no more than 10°), with the third midway between. In the table, the two minima connected by each transition state are given, as are the dihedral angles of the transition state structure.

On the basis of the experimental and calculated results for 5PPene, a model for its isomerization emerges. First, each pair of minima is connected to one another by many pathways, several of which may have similar rate-limiting barriers. As a result, the notion of a single preferred pathway from reactant to product is not appropriate. Second, both the experimental bounds on the barriers and the calculated transition states in Table 3 point toward a two-tier barrier model, in which the τ_3 barrier that controls the vinyl group orientation is ∼600 cm^{-1}, while all the other isomerizations that involve the $C_\alpha-C_\beta$ and $C_\beta-C_\gamma$ alkyl chain motions are approximately twice this size (∼1200 cm^{-1}). Thus, below 600 cm^{-1} internal energy, the low-energy conformers of 5PPene cannot isomerize. Between 600 and 1200 cm^{-1}, only the vinyl group can reorient, and this only between the two low-lying minima, eclipsed with either of the CH groups in the adjoining C_γ. However, as Tables 2 and 3 show, above the ∼1200 cm^{-1} threshold, barriers separating all five conformational minima are overcome essentially all at once, opening up a much larger phase space for exploration at these energies and above. This sharp onset for isomerization involving hindered rotation of the alkyl chain is reflected in the

reactant−reactant spectra, which all show a sharp decline in gain signal at a threshold of 1000−1200 cm^{-1}, reflecting the fact that the initially excited population suddenly has access at these energies to all five conformational minima, and therefore spreads its population over these minima. Finally, the fact that the barriers out of A (1200−1374 cm^{-1}) are slightly larger than the threshold decreases in the reactant SEP-PT scans out of B−E (1000−1200 cm^{-1}) probably reflects the fact that conformer A is the global minimum, with the less stable structures having smaller barriers to isomerization by virtue of being higher in energy. This is consistent with the similar sizes of the S_0-S_1 origin transitions for A−E in the R2PI spectrum. We thus surmise that all five observed conformers of 5PPene have zero-point energies that are likely to be within ∼200 cm^{-1} of one another in energy. Unfortunately, only the B↔C pair provide any direct constraint on the relative energies of the minima, but these two showed similar near-threshold behavior, indicating that these minima are very similar in energy. The five conformational minima thus have small energy separations compared to the largest barriers separating them, which land either in the 600 cm^{-1} region if the vinyl group alone is involved or in the ∼1200 cm^{-1} range whenever the alkyl chain participates. The calculated barriers in the 1650−1850 cm^{-1} range in Table 3 arise from steric hindrance between either two segments of the side chain or between the chain and the aromatic ring.

Theoretical modeling of the rates of isomerization and exploration of the possibility for nonstatistical isomerization dynamics will need to take the unique corrugation of this potential energy surface into account. Ideally, measurements like the ones contained in this study could be used also to extract energy-dependent isomerization rates between individual X→Y conformer pairs. Doing so would require some knowledge of the rate of vibrational cooling that acts in competition with isomerization above threshold. Unfortunately, the experimental limitations already noted for 5PPene (low oscillator strength and sparse SEP spectrum) currently prevent a more quantitative study of this type. However, such studies are beginning to appear,[14] and hold out promise for future work that can provide quantitative data on the isomerization rates as a function of energy above threshold.

V. Conclusions

SEP-PT spectroscopy has been used to place bounds on the lowest energy isomerization barriers separating 14 X→Y reactant−product conformer pairs in 5-phenyl-1-pentene. Three of the measured thresholds are associated with hindered rotation about one of the single C−C bonds in the pentene chain (dihedrals τ_1, τ_2, τ_3, Figure 1). The lowest energy barrier involves hindered rotation about the C−C(vinyl) bond (τ_3), with a barrier just below 620 cm^{-1} separating the two stable orientations of the vinyl group, eclipsed with either of the two adjacent methylene CH bonds. The two alkyl C−C bonds (τ_1, τ_2) both have barriers between 1200 and 1374 cm^{-1}. Above this threshold, conformer A (the ggH_γ' conformer) can isomerize to any of the other four observed conformers.

The body of data is consistent with the elementary notion that isomerization on this multidimensional torsional surface occurs by a sequential set of rotations about single C−C bonds. At energies below 600 cm^{-1}, isomerization is not possible. Between 600 and 1200 cm^{-1}, isomerization is restricted to that involving τ_3, which reorients the terminal vinyl group. Because the individual barriers for hindered rotation of the alkyl C−C bonds are similar, above ∼1200−1400 cm^{-1}, a large region of the torsional potential energy surface opens up, with facile isomerization between all five observed conformers. One would anticipate that a similar single energy threshold would dominate isomerization in longer alkyl chains, with a dramatic shift from highly restricted to fully fluxional occurring in a relatively narrow energy range. Under such circumstances, a multiplicity of isomerization pathways all contributing to the isomerization between individual conformer wells would be predicted.

Acknowledgment. This work was supported by the Department of Energy Basic Energy Sciences, Division of Chemical Sciences under Grant No. DE-FG02-96ER14656. GridChem (http:www.gridchem.org) [R. Dooley, G. Allen, and S. Pamidighantam: Computational Chemistry Grid: Production Cyberinfrastructure for Computational Chemistry; Proceedings of the 13th Annual Mardi Gras Conference, Baton Rouge, LA, Feb 2005, p 83. K. Milfeld, C. Guiang, S. Pamidighantam, J. Giuliani: Cluster Computing through an Application-oriented Computational Chemistry Grid; Proceedings of the 2005 Linux Clusters: The HPC Revolution, Apr 2005] is acknowledged for computational resources and services for the selected results used in this publication.

References and Notes

(1) Pillsbury, N. R.; Zwier, T. S. *J. Phys. Chem. A* **2008**, *113*, 118.
(2) Hammonds, K. D.; McDonald, I. R.; Ryckaert, J. P. *Chem. Phys. Lett.* **1993**, *213*, 27.
(3) Ryckaert, J. P.; Bellemans, A. *Chem. Phys. Lett.* **1975**, *30*, 123.
(4) Cassol, R.; Ferrarini, A.; Nordio, P. L. *J. Phys.: Condens. Matter* **1994**, *6*, A279.
(5) Brown, F. L. H. *Annu. Rev. Phys. Chem.* **2008**, *59*, 685.
(6) Efremov, R. G.; Nolde, D. E.; Konshina, A. G.; Syrtcev, N. P.; Arseniev, A. S. *Curr. Med. Chem.* **2004**, *11*, 2421.
(7) Roubaud, A.; Lemaire, O.; Minetti, R.; Sochet, L. R. *Combust. Flame* **2000**, *123*, 561.
(8) Tancell, P. J.; Rhead, M. M.; Pemberton, R. D.; Braven, J. *Fuel* **1996**, *75*, 717.
(9) Clarkson, J. R.; Baquero, E.; Shubert, V. A.; Myshakin, E. M.; Jordan, K. D.; Zwier, T. S. *Science* **2005**, *307*, 1443.
(10) Clarkson, J. R.; Baquero, E.; Zwier, T. S. *J. Chem. Phys.* **2005**, *122*, 214312.
(11) Clarkson, J. R.; Dian, B. C.; Moriggi, L.; DeFusco, A.; McCarthy, V.; Jordan, K. D.; Zwier, T. S. *J. Chem. Phys.* **2005**, *122*, 214311.
(12) Dian, B. C.; Clarkson, J. R.; Zwier, T. S. *Science* **2004**, *303*, 1169.
(13) LeGreve, T. A.; Clarkson, J. R.; Zwier, T. S. *J. Phys Chem. A* **2008**, *112*, 3911.
(14) Pillsbury, N. R.; Zwier, T. S. Submitted for publication, 2008.
(15) Selby, T. M.; Clarkson, J. R.; Mitchell, D.; Fitzpatrick, J. A. J.; Lee, H. D.; Pratt, D. W.; Zwier, T. S. *J. Phys Chem. A* **2005**, *109*, 4484.
(16) Selby, T. M.; Zwier, T. S. *J. Phys Chem. A* **2007**, *111*, 3710.
(17) Becke, A. D. *Phys. Rev. A* **1988**, *38*, 3098.
(18) Lee, C. T.; Yang, W. T.; Parr, R. G. *Phys. Rev. B* **1988**, *37*, 785.
(19) Zhao, Y.; Schultz, N. E.; Truhlar, D. G. *J. Chem. Theory Comput.* **2006**, *2*, 364.
(20) Pillsbury, N. R.; Müller, C. W.; Plusquellic, D. F.; Zwier, T. S. *J. Chem. Phys.* **2008**, *129*, 114301.
(21) Frisch, M. J.; Head-Gordon, M.; Pople, J. A. *Chem. Phys. Lett.* **1990**, *166*, 275.
(22) Frisch, M. J.; Head-Gordon, M.; Pople, J. A. *Chem. Phys. Lett.* **1990**, *166*, 281.
(23) Head-Gordon, M.; Head-Gordon, T. *Chem. Phys. Lett.* **1994**, *220*, 122.
(24) Head-Gordon, M.; Pople, J. A.; Frisch, M. J. *Chem. Phys. Lett.* **1988**, *153*, 503.
(25) Moller, C.; Plesset, M. S. *Phys. Rev.* **1934**, *46*, 0618.
(26) Sæbo, S.; Almlöf, J. *Chem. Phys. Lett.* **1989**, *154*, 83.
(27) Frisch, M. J.; Trucks, G. W.; Schlegel, H. B.; Scuseria, G. E.; Robb, M. A.; Cheeseman, J. R.; Montgomery, J. A., Jr.; Vreven, T.; Kudin, K. N.; Burant, J. C.; Millam, J. M.; Iyengar, S. S.; Tomasi, J.; Barone, V.; Mennucci, B.; Cossi, M.; Scalmani, G.; Rega, N.; Petersson, G. A.; Nakatsuji, H.; Hada, M.; Ehara, M.; Toyota, K.; Fukuda, R.; Hasegawa, J.; Ishida, M.; Nakajima, T.; Honda, Y.; Kitao, O.; Nakai, H.; Klene, M.; Li, X.; Knox, J. E.; Hratchian, H. P.; Cross, J. B.; Bakken, V.; Adamo, C.; Jaramillo, J.; Gomperts, R.; Stratmann, R. E.; Yazyev, O.; Austin, A. J.; Cammi, R.; Pomelli, C.; Ochterski, J. W.; Ayala, P. Y.; Morokuma, K.; Voth, G. A.; Salvador, P.; Dannenberg, J. J.; Zakrzewski, V. G.; Dapprich, S.; Daniels, A. D.; Strain, M. C.; Farkas, O.; Malick, D. K.; Rabuck, A. D.;

Raghavachari, K.; Foresman, J. B.; Ortiz, J. V.; Cui, Q.; Baboul, A. G.; Clifford, S.; Cioslowski, J.; Stefanov, B. B.; Liu, G.; Liashenko, A.; Piskorz, P.; Komaromi, I.; Martin, R. L.; Fox, D. J.; Keith, T.; Al-Laham, M. A.; Peng, C. Y.; Nanayakkara, A.; Challacombe, M.; Gill, P. M. W.; Johnson, B.; Chen, W.; Wong, M. W.; Gonzalez, C.; Pople, J. A. *Gaussian 03*, Revision E.01; Gaussian, Inc.: Wallingford, CT, 2004.

(28) Hopkins, J. B.; Powers, D. E.; Mukamel, S.; Smalley, R. E. *J. Chem. Phys.* **1980**, *72*, 5049.

(29) Hopkins, J. B.; Powers, D. E.; Smalley, R. E. *J. Chem. Phys.* **1980**, *72*, 5039.

(30) Hopkins, J. B.; Powers, D. E.; Smalley, R. E. *J. Chem. Phys.* **1980**, *73*, 683.

(31) Baer, T.; Hase, W. L. *Unimolecular Reaction Dynamics: Theory and Experiments*; Oxford University Press: Oxford, UK, 1996.

(32) Marcus, R. A. *J. Chem. Phys.* **1952**, *20*, 359.

(33) Lubman, D. M.; Rettner, C. T.; Zare, R. N. *J. Phys. Chem.* **1982**, *86*, 1129.

(34) Shields, A. E.; van Mourik, T. *J. Phys Chem. A* **2007**, *111*, 13272.

(35) Zhao, Y.; Truhlar, D. G. *Acc. Chem. Res.* **2008**, *41*, 157.

(36) Benighaus, T.; DiStasio, R. A.; Lochan, R. C.; Chai, J. D.; Head-Gordon, M. *J. Phys Chem. A* **2008**, *112*, 2702.

(37) Chai, J. D.; Head-Gordon, M. *J. Chem. Phys.* **2008**, *128*, 084106.

(38) Grimme, S. *J. Chem. Phys.* **2006**, *124*, 034108.

(39) Zhao, Y.; Truhlar, D. G. *J. Chem. Theory Comput.* **2007**, *3*, 289.

(40) Baquero, E. E.; James, W. H., III; Choi, T. H.; Jordan, K. D.; Zwier, T. S. *J. Phys. Chem. A* **2008**, *112*, 11115.

(41) Emery, R.; Macleod, N. A.; Snoek, L. C.; Simons, J. P. *Phys. Chem. Chem. Phys.* **2004**, *6*, 2816.

(42) Mons, M.; Piuzzi, F.; Dimicoli, I. *Actual. Chim.* **2007**, *314*, 19.

(43) Snoek, L. C.; Kroemer, R. T.; Hockridge, M. R.; Simons, J. P. *Phys. Chem. Chem. Phys.* **2001**, *3*, 1819.

(44) Zwier, T. S. *J. Phys Chem. A* **2006**, *110*, 4133.

(45) Zwier, T. S. *J. Phys Chem. A* **2001**, *105*, 8827.

(46) Korth, M.; Luechow, A.; Grimme, S. *J. Phys Chem. A* **2008**, *112*, 2104.

(47) Schwabe, T.; Grimme, S. *Phys. Chem. Chem. Phys.* **2007**, *9*, 3397.

JP806699E